Desalination and Water Treatment
www.deswater.com

doi:10.5004/dwt.2016.0097

59 (2017) 210–219
January

Adsorption of methylene blue onto acid-treated mango peels: kinetic, equilibrium and thermodynamic study

Ali H. Jawad[a,b*], N.F. Hanani Mamat[b], Mohd Fauzi Abdullah[b], Khudzir Ismail[a]

[a]*Coal and Biomass Energy Research Group, Faculty of Applied Sciences, Universiti Teknologi, MARA, 40450 Shah Alam, Selangor, Malaysia, Tel. +60 49882571; email: ali288@perlis.uitm.edu.my, ahjm72@gmail.com (A.H. Jawad), Tel. +60 355444562; email: khudzir@salam.uitm.edu.my (K. Ismail)*
[b]*Coal and Biomass Energy Research Group, Faculty of Applied Sciences, Universiti Teknologi, MARA, Arau Campus, 02600 Arau, Perlis, Malaysia, Tel. +60145050781; email: nanihanani49@yahoo.com (N.F.H. Mamat), Tel. +60 49882737 email: mohdfauziabd@perlis.uitm.edu.my (M.F. Abdullah)*

Received 24 January 2016; Accepted 17 June 2016

ABSTRACT

Mango (Mangifera indica L.) peel, an abundant residue of the food industry and kitchen waste, was used as an alternative source of activated carbon. In this work, mango peels activated carbon (MPAC) was prepared by chemical activation with H_2SO_4. The physical properties of the MPAC were evaluated through the bulk density, ash content, moisture content, and iodine number. The surface characterization of MPAC was achieved using fourier transform infrared (FTIR), scanning electron microscopy (SEM), and the point of zero charge (pH_{PZC}) method. Batch experiments were carried out for the adsorption of methylene blue (MB) onto MPAC surface. The operating variables studied were adsorbent dose, initial solution pH, initial dye concentration and contact time, and temperature. Langmuir, Freundlich, and Temkin isotherms were used to analyze the equilibrium data at 303 K. The kinetic uptake profiles are well described by the pseudo-second-order model, and the Langmuir model describes the adsorption behaviour at equilibrium. The maximum adsorption capacity of MPAC with methylene blue was 277.8 mg g^{-1}. Various thermodynamic parameters such as standard enthalpy (ΔH^o), standard entropy (ΔS^o) and standard free energy (ΔG^o) showed that the adsorption of MB onto MPAC was favourable and endothermic in nature. Thus, this study demonstrated the potential of using mango peels waste as cheap and efficient raw materials to produce activated carbon for MB removal.

Keywords: Mango peels; Activated carbon; Methylene blue; Adsorption; Biomass; Activation

1. Introduction

Effluents generated from dyeing industries, such as textile and printing, have been identified as emerging environmental problems in aquatic environments. Most of these dyes are highly visible, stable and resistant to chemical, photochemical as well as biological degradation. Besides, they are often toxic and carcinogenic due to their complex aromatic structure and synthetic nature [1]. Many treatment methods for the removal of dyes from industrial effluents include adsorption [2], bioremediation [3], electrochemical degradation [4], cation exchange membranes [5], Fenton chemical oxidation [6], photocatalysis [7,8], and anaerobic microbial treatment [9]. Among the various water treatment methods, adsorption is one of the most effective treatment techniques for advanced wastewater treatment to reduce hazardous waste pollutants in effluent. Adsorption-based treatment with appropriate adsorbent materials displays high performance and selectivity, flexibility and simplicity of design, convenience of operation without producing harmful by-products [10].

Activated carbon (AC) is a widely used industrial carbonaceous adsorbent due to its high surface area, variable pore structure, high adsorption capacity and occurrence of various surface functional groups, according to the mode of

*Corresponding author.

preparation. AC can remove a wide variety of pollutants such as dyes, heavy metals, pesticides and gases. Carbonaceous solid precursors from natural or synthetic sources can be used to produce activated carbon [11]. Research and development of carbonaceous adsorbents from agricultural waste peels is an area of ongoing interest because the precursors are eco-friendly, cheap, renewable, safe, and abundant. In recent years, researchers have studied the production of ACs from fruit and vegetable peels as cheap and renewable precursors, such as orange peel [12,13], Jackfruit peel [14], Mangosteen peel [15], pineapple peel [16], Citrus fruit peel [17], potato peel [18], rambutan peel [19], pomegranate peel [20], grapefruit peel [21], cassava peel [22], Cucumis sativus peel [23], pomelo peel [24], banana peel [25], guava peel [26], mandarin peel [27].

Mango (Mangifera indica L.) is a fruit that grows abundantly in 85 different countries and is considered one of the most important tropical fruit in the world since its consumption corresponds to 50% of the entire consumption of all tropical fruits. Around 35 to 60% of the total mass of processed fruits is considered by-products, which are discarded in landfills without any commercial purpose [28,29]. From literature, it is known that the mango peel contains different phytochemicals like polyphenols, carotenoids, vitamin E, lactic acid, dietary fibres and vitamin C and it also exhibited good antioxidant properties [30–32]. These previous studies encourage us to find another useful utilization of mango peel as a new, low-cost and renewable precursor for preparing activated carbon as an adsorbent. The reuse of this great mass of natural waste product represents an important opportunity from both environmental and socioeconomic points of view.

The Mango by-products are considered a residue without a destination in the processing industries. These easily obtained and eco-friendly by-products had been employed as an ideal alternative to the current expensive adsorbents of removing dyes from wastewater such as mango seed [33–35]. Recently, many researches have been performed with the aim of producing low cost ACs from mango by-products as a renewable source [36,37]. The adsorption property of activated carbon strongly depends on the activation procedures, which are physical (thermal) activation or chemical activation, and the nature of source materials [38]. Among various chemical activation agents, sulphuric acid is frequently used as a low cost activator for the preparation of carbon adsorbents from lignocellulosic products. H_2SO_4 gives the possibility to develop porous structure by degrading of cellulosic material in plant materials and the aromatization of the carbon skeleton [39].

Therefore, the focus of this study was to develop a low-cost AC adsorbent from mango peel with H_2SO_4 activation. The textural and chemical characterizations of the acid-treated mango peel activated carbon (MPAC) were also performed. The adsorption properties of MPAC were evaluated in the removal of a basic dye, methylene blue (MB) from aqueous solutions. In order to establish the removal capacity of this adsorbent, different models of isotherms and adsorption kinetics were fitted to the experimental data. To the best of our knowledge, this work is the first reported example of the use of mango peel as a precursor for preparing AC via chemical activation with H_2SO_4.

2.Materials and methods

2.1. Adsorbate (MB)

Methylene blue (MB) supplied by R&M Chemicals, Malaysia was used as an adsorbate. Ultra-pure water was used to prepare all solutions. MB has a chemical formula ($C_{16}H_{18}ClN_3S.xH_2O$) and molecular weight (319.86 g mol^{-1}).

2.2. Preparation of activated carbon

Mango peel (MP) of golden dragon variety used for preparation of activated carbon was collected from the local fresh juice shop in Penang, Malaysia. MP was firstly washed with water and subsequently dried at 105°C for 24 h to remove the moisture contents. The dried MP was ground and sieved to the size of 1–2 mm before mixing with concentrated H_2SO_4 (95–98%). The mixing ration was fixed at 1 g of dried MP powder with 1 mL of concentrated H_2SO_4 according to the method reported by Garg et al. [40]. The obtained activated carbon MPAC was ground and sieved to obtain a powder with a particle size range of 150–212 µm. The yield of MPAC was calculated according to a published method [41]. The bulk or apparent density was determined by following the method reported by Ahmedna et al. [42]. The moisture content was determined by an oven drying method [43], where the ash content determination used standard methods [44]. The iodine number is a measure of micropore content (0–20Å) and was obtained by a standard method [45]. The proximate analysis of the MPAC was carried out using a muffle furnace. The surface morphology of MPAC before and after adsorption of MB was measured using a scanning electron microscope (SEM; SEM-EDX, FESEM CARL ZEISS, SUPKA 40 VP). The functional groups of MPAC before and after MB adsorption were measured via fourier transform infrared (FTIR) spectroscopy (PerkinElmer, Spectrum RX I) in transmission mode with a spectral range from 4000 to 400 cm^{-1} with a resolution of 4 cm^{-1}. All samples were prepared with spectroscopic grade KBr which constituted ~80% (w/w) of the total sample and were run as finely ground powders. The pH at the *point-of-zero* charge (pHPZC) was estimated by using a pH meter (Metrohm, Model 827 pH Lab, Switzerland), as described elsewhere [46]. In this method, the pH of a suspension of the MPAC (0.15 mg) in a NaCl aqueous solution (50 mL at 0.01 mol L^{-1}) was adjusted to successive initial values between 2 and 12. The suspensions were stirred 48 h and the final pH was measured and plotted versus the initial pH. The pHPZC is determined at the value for which $pH_{final} = pH_{initial}$. The elemental analysis was carried out using an elemental analyser CHNS-O, model Flash 2000 analyser.

2.3. Batch adsorption experiments

The batch adsorption experiments of MB onto MPAC were carried out in a series of 250 mL Erlenmeyer flasks containing 100 mL of MB solution. The flasks were capped and agitated in an isothermal water bath shaker (Memmert, waterbath, model WNB7-45, Germany) at fixed shaking speed of 110 stroke min^{-1} and 303 K until equilibrium was attained. Batch adsorption experiments were carried

out by varying several experimental variables such as adsorbent dosage (0.2 to 2.0 g L^{-1}), pH (3 to 10), initial dye concentration (25 to 400 mg L^{-1}) and contact time (0 to 900 min.) to determine the optimum uptake conditions for adsorption. The pH of MB solution was adjusted by adding either 0.10 M HCl or NaOH. After mixing of the MPAC-MB system, the supernatant was collected with a 0.20 µm Nylon syringe filter and the concentrations of MB were monitored at a different time interval using a HACH DR 2800 Direct Reading Spectrophotometer at the maximum wavelength (λ_{max}) of absorption at 661 nm. For the thermodynamic studies, similar procedures were applied at 313 K and 323 K, with the other variables held constant. The blank test was carried out in order to account for color leached by the adsorbent and adsorbed by the glass containers, blank runs with only the adsorbents in 100 mL of doubly distilled water and 100 mL of dye solution without any adsorbent were conducted simultaneously at similar conditions. The adsorption capacity at equilibrium, q_e (mg g^{-1}) and the percent of color removal, *CR* (%) of MB were calculated using Eqs. (1) and (2).

$$q_e = \frac{(C_0 - C_e)}{W} V \quad (1)$$

$$CR\% = \frac{(C \quad C)}{} \times 100 \quad (2)$$

C_0 is the initial dye concentration (mg L^{-1}); C_e is the dye concentration at equilibrium (mg L^{-1}); V is the volume of dye solution (L); and W is the dry mass of the adsorbent (mg). Adsorption experiments were conducted in triplicate under identical conditions and the results are reported as an average value.

3. Results and discussion

3.1. Characterization of MPAC

The results of physical characterization of MPAC are recorded in Table 1. The results indicate that MPAC has a moderate iodine number, low values of bulk density, ash content and moisture content, along with a relatively high yield of carbon. The pHpzc of the MPAC was 4.60, which indicates the acid character of the MPAC surface. The surface morphology of MPAC adsorbent was evaluated according to the SEM images obtained in Fig. 1. There is a change in surface morphology of the MPAC powder before (Fig. 3a) and after the adsorption (Fig. 3b) of MB. According to (Fig. 1a), the surface features of MPAC are well-pronounced heterogeneous cavities that well-distributed across the MPAC surface. Therefore, the SEM image reveals that MB may be adsorbed onto the MPAC surface and the accessible pore domains of the carbonaceous surface. The surface morphology of MPAC after MB adsorption reveals a change in the topography of the adsorbent, as evidenced by the appearance of reduced pore structure and smoother surface features due to the adsorption of MB in (Fig. 1b). The pattern of adsorption onto biomass materials is related to the availability of active functional groups and bonds of the AC surface. For the elucidation of these active sites, FTIR spectral analysis was performed. Several IR bands appearing in the FTIR spectrum of MPAC before adsorption (Fig. 2a) that were assigned to various functional groups, in accordance with their respective wavenumber (cm^{-1}) position as reported in literature. The region between 3600 cm^{-1} and 2600 cm^{-1} indicates two major IR bands, where a broad and strong band stretch are observed from 3600 cm^{-1} to 3000 cm^{-1}. The latter indicates the presence of free or hydrogen bonded O–H groups (alcohols, carboxylic acids and phenols) as in pectin, cellulose and lignin on the surface of the adsorbent [47]. The O–H stretching vibrations occur within a broad range of frequencies indicating the presence of "free" hydroxyl groups and bonded O–H bands such as carboxylic acids. The weak band observed from 2900 cm^{-1} to 2750 cm^{-1} is assigned to the aliphatic C–H stretching (methine, methyl, and methylene groups of side chains) and from aromatic C–H stretching near 3100 cm^{-1}. The band at about 1700 cm^{-1} relates to C=O stretching of ketones, aldehydes, lactones or carboxyl groups, and the band at 1600–1580 cm^{-1} is assigned to C=C vibrations in aromatic rings [48]. The IR bands between 1300 and 1000 cm^{-1} are observed for oxidized carbon materials and are assigned to C–O and/or C–O–C stretching in acids, alcohols, phenols, ethers and/or esters groups, and sulphonic acid groups ($–SO_3$). Thus, the FTIR spectrum of MPAC before adsorption (Fig. 2a) indicates that the external surface of MPAC is rich in functional groups, containing oxygen of carboxylic, carbonyl and phenolic species. After adsorption of MB, the spectrum of MPAC (Fig. 2b) shows attenuated band intensity where the functional groups either shifted in frequency or became more pronounced as shown at 1650 cm^{-1} (–N–H bending) and at 1350 cm^{-1} (C–N vibration of amide) suggested the interactions of MB molecules with the functional groups of MPAC.

Table 1
Physicochemical characteristics of the activated carbon (MPAC)

Typical properties	
Bulk density (g mL^{-1})	0.67
Iodine number (mg g^{-1})	244.2
pHpzc	4.60
Proximate analysis (wt. %)	
Ash content	5.84
Moisture content	12.23
Fixed carbon (yield)	67.35
Volatile matter	14.58
Ultimate analysis (wt.%)	
C	51.84
H	3.66
N	Not detected
S	0.85
O (by difference)	43.63

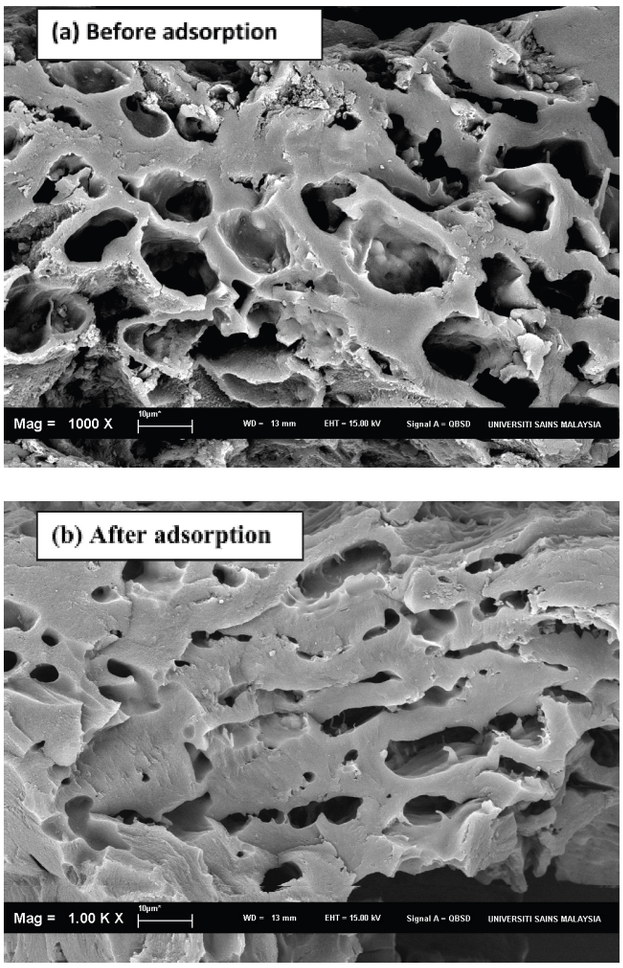

Fig. 1. SEM micrograph of MPAC particle (1000x magnification): (a) before MB adsorption and (b) after MB adsorption.

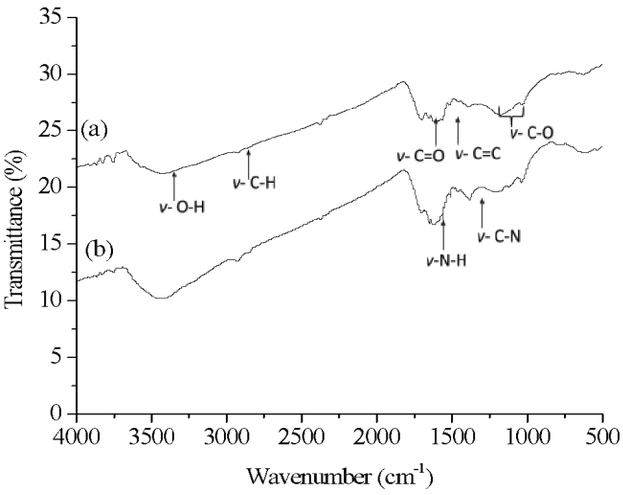

Fig. 2. FTIR spectra of PMAC (a) before adsorption and (b) after MB adsorption (b).

3.2. MB adsorption

3.2.1. Effect of the PMAC mass

The effect of MPAC mass on the removal of the MB from aqueous solution was performed by using variable quantities (0.020 to 0.20 g) of MPAC at fixed volumes (100 mL) and initial dye solution where C_o was 100 mg L^{-1}. For these experiments, other operation parameters were held constant at 303 K, shaking speed of 110 stroke min^{-1}, contact time of 60 min, and an unadjusted pH at 5.60 for the initial MB solution. The results are shown in Fig. 3. It was found that by increasing the mass of PMAC till 0.14 g the removal percentage increased rapidly and further addition has not significantly affected the MB removal percentage. The observed increase in the MB removal (%) with MPAC mass was attributed to an increase in the available adsorbent surface area, as the number of adsorption sites increase correspondingly [49]. However, no significant changes in MB removal efficiency were observed beyond 0.14 g 100 mL^{-1} MPAC dose. Due to conglomeration of adsorbent particles, there is no increase in effective surface area of MPAC. Therefore, 0.14 g of MPAC was selected for subsequent work.

3.2.2. Effect of pH

The pH of the solution influences the association of counter ions with MB, along with the surface charge of the adsorbent. Fig. 4 shows the effect of variable pH from 3.0 to 10.0 on the adsorption capacity with MB. The adsorption capacity of MB onto MPAC increased when the pH increased from 3.0 to 5.0, where no remarkable change was observed by increasing the pH to an alkaline environment. Lower adsorption of MB at acidic pH can be due to the competition of excess H^+ ions with MB cations for potential adsorption sites [50]. On the other hand, at higher pH, the surface of MPAC may adopt negative surface charge which enhances adsorption of cation species through attractive electrostatic attractions, contributing to an increase in the rate of adsorption [50]. Moreover, the surface of the adsorbent was positively charged, since the pH < pHPZC = (4.60), contributing to repulsion of MB cations. The optimum pH for the removal of MB by MPAC is at pH 5.0~6.0.

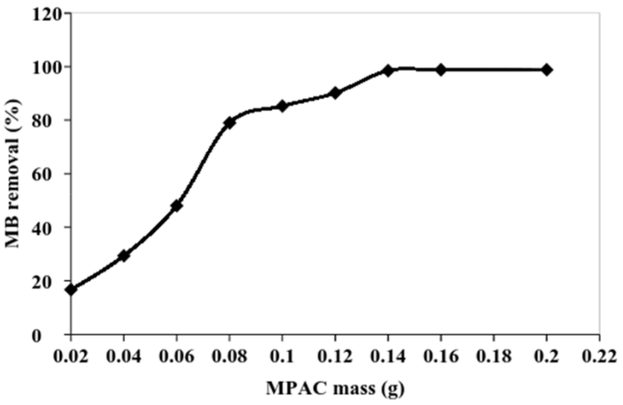

Fig. 3. The effect of MPAC mass on the MB removal (%) at [MB] o = 100 mg L^{-1}, V = 100 mL, unadjusted pH = 5.60, T = 303 K, shaking speed = 110 stroke min^{-1}, and contact time = 60 min.

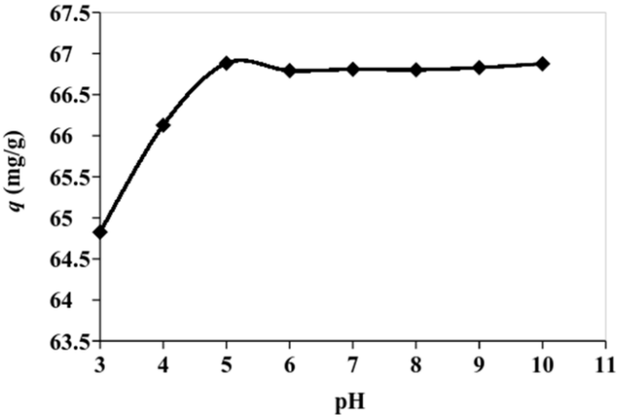

Fig. 4. The effect of pH on the MB uptake using 0.14 g of MPAC, $[MB]_o$ = 100 mg L^{-1}, V = 100 mL, T = 303 K, shaking speed = 110 stroke min^{-1}, and contact time = 60 min.

In this regard, it was found that the pH value of the original MB solution is 5.6 and lies within the optimal pH range. In order to reduce chemicals consumption as well as labor requirements, therefore the pH value of unadjusted MB solution (pH 5.6) was used for this study.

3.2.3. Effect of initial dye concentration and contact time

The experimental results for the adsorption properties of MB onto MPAC at various initial concentrations are shown in Fig. 5. The amount of MB adsorbed by the MPAC adsorbent at equilibrium increased rapidly from 9.60 to 265.50 mg g^{-1} as the initial dye concentration increased from 25 to 400 mg L^{-1}. Indeed, the resistance to mass transfer between the solid and aqueous phase is more easily overcome due the driving forces. Moreover the number of collisions between MB molecules and MPAC is increased, increasing the adsorption. Hence, additional amounts of MB were transferred to the MPAC surface. Additional time was needed to reach equilibrium for higher dye concentration because there was a tendency for MB to penetrate deeper within the interior surface of the MPAC and be adsorbed at active pore sites. This indicates that the initial dye concentration plays a significant role in the adsorption capacity of MB onto MPAC sorbent. Similar observations were reported for the adsorption of MB on the surface of various AC materials obtained from different biomass sources prepared using H_2SO_4 activation [39,51,52].

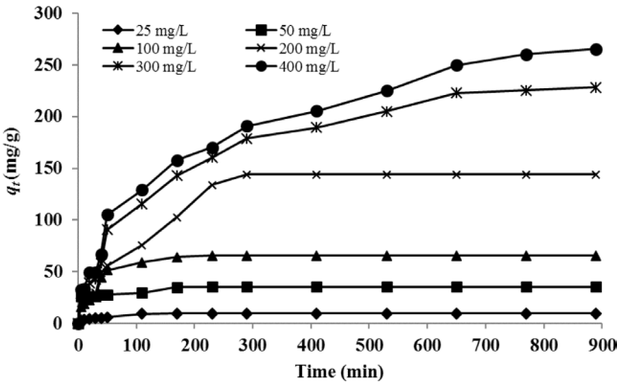

Fig. 5. Effect of contact time and initial concentration on the adsorption of MB by MPAC (V = 100 mL, pH = 5.6, T = 303 K, shaking speed = 110 stroke min^{-1} and MPAC mass = 0.14 g).

3.2.4. Effect of temperature on MB uptake

The effect of temperature on the dye adsorption properties of MPAC adsorbent at 303, 313 and 323 K with fixed initial MB concentration of 200 mg L^{-1} was investigated, as shown in Fig. 6. The uptake of methylene blue onto activated carbon was rapid initially and then slows down gradually until it attained equilibrium beyond which there was not significantly increased in the MB uptake. The adsorption capacity of the MPAC increased from 144.1 to 164.2 mg g^{-1} as the temperature increased from 303 to 323 K. The observed results in Fig. 6 indicate that the adsorption process of MB onto MPAC was favored at higher temperature, in agreement with an endothermic adsorption process. The fact that the MB uptake is favored by temperature indicates that the mobility of the dye molecules increases with a rise in the temperature. It can also be said that reaction of dye molecules and surface functional groups is enhanced by increased temperature of reaction [53].

3.3. Kinetic studies

The pseudo-first-order model (PFO) and pseudo-second-order model (PSO) were used to investigate the adsorption kinetics of MB dye on MPAC. The conformity between experimental data and the model predicted values was expressed by correlation coefficient (R^2). The PFO model of Lagergren [54] is based on solid capacity and generally expressed as follows:

$$\ln(q_e - q) = \ln(q_e) - (k_1)t \quad (3)$$

where q_e is the amount of solute adsorbed at equilibrium per unit weight of adsorbent (mg g^{-1}), q is the amount of sol-

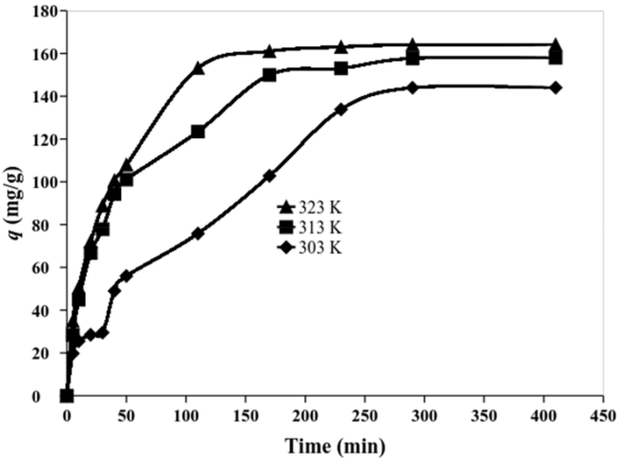

Fig. 6. Effect of temperature on the equilibrium adsorption capacity of MPAC at $[MB]_o$ = 200 mg L^{-1}, V = 100 mL, pH = 5.6, shaking speed = 110 stroke min^{-1} and MPAC mass = 0.14 g.

ute adsorbed at any time (mg g^{-1}), and k_1 is the adsorption constant. This expression is the most popular form of pseudo-first-order kinetic model. k_1 values at different initial MB concentrations were calculated from the plots of $\ln(q_e–q)$ versus t and the values are given in Table 2. The correlation coefficient (R^2) values obtained were relatively low; hence, this model has very poor correlation coefficients (R^2) for the best fit data. Thus, the kinetic data were analyzed using the PSO model [55], which can be expressed as follows:

$$\frac{t}{q}=\left(\frac{1}{k_2q_e^2}\right)+\left(\frac{1}{q_e}\right)t \tag{4}$$

The plot of t/q versus t should give a linear relationship, from which q_e and k_2 can be determined from the slope and intercept of the plot. The PSO rate constant (k_2, g mg^{-1} min^{-1}) and $q_{e'cal}$ were calculated from the intercept and slope of t/q_t versus t. The kinetic adsorption results of MB by MPAC under various conditions were calculated from the related plots and the results are listed in Table 2. Based on the given data, the adsorption of MB dye perfectly followed the PSO model.

3.4. Adsorption isotherm studies

Adsorption isotherm reveals the relationship between the mass of adsorbate adsorbed per unit weight of adsorbent at equilibrium and liquid-phase equilibrium concentration of the adsorbate [46]. To quantify the adsorption capacity of MPAC for the removal of MB dye from aqueous solutions, we tested the Langmuir, Freundlich, and Temkin isotherm models. The Langmuir model assumes that the adsorptions occur at specific homogeneous sites on the adsorbent. Langmuir model is successfully used in numerous monolayer adsorption processes [56]. The data of the equilibrium studies for the adsorption of MB dye onto MPAC may follow the Langmuir model as follows:

$$\frac{C_e}{q_e}=\frac{1}{q_mK_L}+\frac{1}{q_m}C_e \tag{5}$$

where C_e is the equilibrium concentration (mg L^{-1}) and q_e is the amount adsorbed (mg) per amount of adsorbent (g), K_L is the Langmuir equilibrium constant, and q_m is the amount of adsorbate required to form a monolayer. Hence, a plot of C_e/q_e versus C_e should be a straight line with a slope ($1/q_m$) and an intercept as ($1/q_m$ K_L), the calculated values are given in Table 3. The Langmuir type adsorption isotherm indicates the surface homogeneity of the adsorbent. The adsorbent surface is made up of small adsorption patches, which are energetically equivalent to each other in terms of adsorption phenomenon. The correlation coefficient (R^2) value of 0.9957 revealed that the adsorption data of MB dye onto MPAC well fitted to the Langmuir isotherm. Moreover, the Freundlich model can be applied for non-ideal adsorption on heterogeneous surfaces and multilayer adsorption [57]. This model is presented as follows:

$$q_e=\left(K_F\right)\left(C_e^{\frac{1}{n}}\right) \tag{6}$$

$$\ln q_e=\ln K_F+\frac{1}{n}\ln C_e \tag{7}$$

Table 3
Isotherm parameters for removal of MB by MPAC at 303K

Isotherm	Parameter	Value
Langmuir	q_m (mg g^{-1})	277.8
	K_L (L mg^{-1})	0.57
	R^2	0.9957
Freundlich	K_F ((mg g^{-1}) (L $mg^{-1})^{1/n}$)	69.34
	n	2.34
	R^2	0.803
Temkin	K_T (L mg^{-1})	5.85
	B	52.64
	R^2	0.8817

Table 2
Comparison of the pseudo-first-order (PFO) and pseudo-second-order (PSO) models for the adsorption of MB on MPAC at 303 K

Parameters	Co (mg L^{-1})					
	25	50	100	200	300	400
$q_{e,\,exp.}$ (mg g^{-1})	9.60	35.47	65.66	144.04	232.44	265.45
PFO						
$q_{e\,cal.}$ (mg g^{-1})	7.90	13.70	53.19	97.10	194.16	241.94
k_1(1 m^{-1})	0.0165	0.0099	0.0162	0.0038	0.0051	0.0033
R^2	0.9032	0.8694	0.9432	0.9414	0.9968	0.9166
PSO						
$q_{e\,cal.}$ (mg g^{-1})	8.71	31.84	59.88	142.85	243.90	256.41
k_2(g mg^{-1} min^{-1}) × 10^{-5}	289	99.10	39.68	9.47	6.29	4.54
R^2	0.9971	0.9954	0.9968	0.9955	0.9955	0.9954

where K_F is the Freundlich equilibrium constant, n is an empirical constant, and the rest of the terms have the usual significance. Thus, a plot of ln q_e versus ln C_e should be a straight line with a slope $1/n$ and an intercept of ln K_F. The related parameters were calculated, and the results are shown in Table 3. Temkin model [58] considered the effects of indirect adsorbate/adsorbate interactions on adsorption isotherms. The Temkin isotherm was used in the following form:

$$q_e = \left(\frac{RT}{b}\right)\ln\left(K_T C_e\right) \tag{8}$$

This equation can be expressed in its linear form as follows:

$$q_e = B\ln K_T + B\ln C_e \tag{9}$$

where $B = (RT/b)$, a plot of q_e versus ln C_e yielded a linear line, enables to determine the isotherm constants K_T and B. K_T is the Temkin equilibrium binding constant (L mg^{-1}) that corresponds to the maximum binding energy, and constant B is related to adsorption heat. The adsorption heat of all the molecules in the layer is expected to decrease linearly with coverage because of adsorbate/adsorbate interactions. The constants K_T and B as well as the R^2 values are shown in Table 3. The Langmuir model fit the data better than the Freundlich and Temkin models (Table 3). This result is also confirmed by the high R^2 value for the Langmuir model (0.9957) compared with the Temkin (0.8817) and Freundlich (0.803) models. The results reveal that the formation of a surface monolayer of dye molecules occurs for MPAC, where the monolayer adsorption capacity (q_m) for MPAC with MB was compared with other types of H_2SO_4-treated AC adsorbents in Table 4. As can be seen in Table 4, MPAC shows higher adsorption capacity when compared with several ACs developed from various biomasses by using chemical activation with H_2SO_4. Out of eight different ACs, only one AC presents higher adsorption capacity than MPAC. This outstanding adsorption capacity for MB places MPAC as one of the best adsorbents for the MB removal from aqueous solutions.

3.5. Adsorption thermodynamics

The thermodynamic adsorption parameters of MB onto MPAC were computed from the experimental data obtained at 303, 313 and 323 K. Gibb's free energy ($\Delta G°$), enthalpy ($\Delta H°$) and entropy ($\Delta S°$) were calculated using the following equations [64]:

$$\Delta G^o = \Delta H^o - T\Delta S^o \tag{10}$$

$$\Delta G° = -RT\ln k_d \tag{11}$$

The combination of Eqs. (10) and (11) gives:

$$\ln k_d = \frac{\Delta S°}{R} - \frac{\Delta H°}{RT} \tag{12}$$

The distribution coefficient (k_d) was calculated using the following equation:

$$k_d = \frac{q_e}{C_e} \tag{13}$$

where q_e is the concentration of MB adsorbed on MPAC at equilibrium (mg L^{-1}), C_e is the equilibrium concentration of MB in the liquid phase (mg L^{-1}), R is the universal gas constant (8.314 J mol^{-1} K) and T is the absolute temperature (K). The values of $\Delta H°$ and $\Delta S°$ were calculated from the slope and intercept of van't Hoff plots of ln k_d versus $1/T$ respectively (Fig. 7). The thermodynamic parameters are listed in Table 5. The negative values of $\Delta G°$ indicate

Table 4
Comparative of adsorption capacities for MB onto different activated carbons prepared by H_2SO_4 activation

H_2SO_4-treated activated carbons	Adsorbent dosage, g	pH	Temp. (K)	q_{max} (mg g^{-1})	References
Mango peel	0.14 g/100 mL	6	303	277.8	This study
Parthenium hysterophorus	0.4 g/100 mL	7	298	39.68	[51]
Euphorbia rigida	0.2 g/100 mL	6	293	114.45	[39]
Sunflower oil cake	0.2 g/100 mL	6	288	16.43	[59]
Delonix regia pods	0.1 g/50 mL	7	298	23.3	[60]
Pine fruit shell	0.06 g/20 mL	8.5	298	529	[52]
Ficus carica	0.5 g/100 mL	8	298	47.62	[61]
Bagasse	0.4 g/100 mL	9	300–333	49.75–56.50	[62]
Coconut leaves	0.15/100 mL	6	303–323	126.9–149.3	[63]

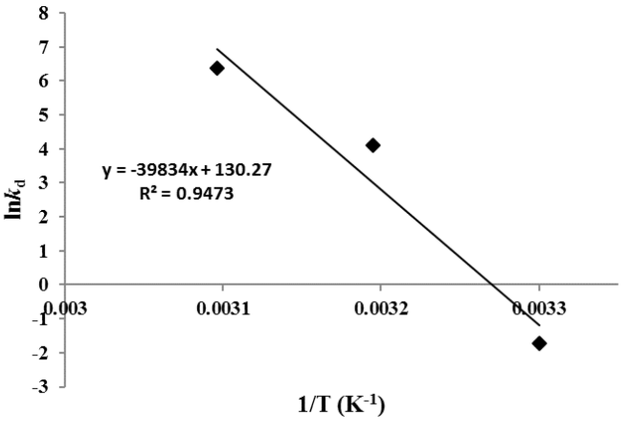

Fig. 7. Plot of ln k_d vs. 1/T for estimation of thermodynamic parameters for the adsorption of MB onto MPAC ($[MB]_o$ = 200 mg L^{-1}, V = 100 mL, pH = 5.6, shaking speed = 110 stroke min^{-1} and MPAC mass = 0.14 g).

Table 5
Thermodynamic parameters values for the adsorption of MB onto MPAC

Temperature (K)	Thermodynamics			
	k_d	$\Delta G°$ (kJ mol^{-1})	$\Delta H°$ (kJ mol^{-1})	$\Delta S°$ (kJ mol^{-1} K)
303	0.18	–75.1		
313	60.78	–76.3	331.2	1.08
323	582.62	–77.5		

spontaneous and favourable methylene blue adsorption onto the surface of MPAC [65]. The positive value of the enthalpy change (ΔH^o = +331.17 kJ mol^{-1}) indicates that the adsorption process is an endothermic and this value also shows that the adsorption follows a chemisorption mechanism in nature involving strong forces of attractions [66]. The positive values of ΔS^o confirm a high preference of MB molecules for the carbon surface of MPAC and also suggest the possibility of some structural changes or readjustments in the dye-carbon adsorption complex [67]. Moreover, it is consistent with the dehydration of dye molecules before its adsorption to carbon surface, and the release of these water molecules to the bulk solution [68].

4. Conclusions

This study investigates the feasibility of mango peel as a new and low-cost precursor for the preparation of activated carbon (MPAC). The results indicate that MPAC is an effective adsorbent for MB adsorption for uptake in dye effluent wastewater streams. This investigation showed that H_2SO_4 treatment could enhance the adsorption capacity of MPAC in removing MB from aqueous solutions. The adsorption experiments indicated that the pseudo-second-order model provided the best description of the kinetic uptake properties. On the other hand, the adsorption isotherms are well described by the Langmuir model where the maximum adsorption capacity (q_m) is 277.8 mg g^{-1}.

Acknowledgment

The authors thank the Faculty of Applied Sciences, Universiti Teknologi MARA, Perils Campus for facilitating this work.

References

[1] G. Crini, P.M. Badot, Application of chitosan, a natural aminopolysaccharide, for dye removal from aqueous solutions by adsorption processes using batch studies: A review of recent literature, Progr. Polym. Sci., 33 (2008) 399–447.
[2] A.H. Jawad, R.A. Rashid, R.M.A. Mahmuod, M.A.M. Ishak, N.N. Kasim, K. Ismail, Adsorption of methylene blue onto coconut (Cocos nucifera) leaf: optimization, isotherm and kinetic studies, Desal. Wat. Treat., 57(19) (2016) 8839–8853.
[3] A.R. Khataee, A. Movafeghi, S. Torbati, S.Y. SalehiLisar, M. Zarei. Phytoremediation potential of duckweed (Lemna minor L.) in degradation of C.I. Acid Blue 92: artificial neural network modeling, Ecotoxicol. Environ. Saf., 80 (2012) 291–298.
[4] L. Fan, Y. Zhou, W. Yang, G. Chen, F. Yang, Electrochemical degradation of aqueoussolution of Amaranth azo dye on ACF under potentiostatic model, Dyes Pigments, 76 (2008) 440–446.
[5] J.S. Wu, C.H. Liu, K.H. Chu, S.Y. Suen, Removal of cationic dye methyl violet 2B from water by cation exchange membranes, J. Membr. Sci. 309 (2008) 239–245.
[6] Y.S. Woo, M. Rafatullah, A.F.M. Al-Karkhi, T.T. Tow, Removal of Terasil Red R dye by using Fenton oxidation: a statistical analysis, Desal. Water Treat., 53 (2013) 1–9.
[7] A.H. Jawad, A.F.M. Alkarkhi, N.S.A. Mubarak, Photocatalytic decolorization of methylene blue by an immobilized TiO_2 film under visible light irradiation: optimization using response surface methodology (RSM), Desal. Water Treat., 56(2015) 161–172.
[8] A.H. Jawad, N.S.A. Mubarak, M.A.M. Ishak, K. Ismail, W.I. Nawawi. Kinetics of photocatalytic decolourization of cationic dye using porous TiO_2 film. J. Taibah Univ. for Sci., 10 (2016) 352–362.
[9] L. Yu, X.Y. Zhang, S. Wanga, Q.W. Tang, T. Xie, N.Y. Lei, Y.L. Chen, W.C. Qiao, W.W. Li, M.H.W. Lam, Microbial community structure associated with treatment of azo dye in a start-up anaerobic sequenced batch reactor, J. Taiwan Inst. Chem. E., 54 (2015) 118–124.
[10] M.J. Ahmad, Application of agricultural based activated carbons by microwave and conventional activations for basic dye adsorption: Review, J. Environ. Chem. Eng., 4 (2016) 89–99.
[11] A.L. Cazetta, A.M.M. Vargas, E.M. Nogami, M.H. Kunita, M.R. Guilherme, A.C. Martins, T.L. Silva, J.G.G. Moraes, V. C. Almeida. NaOH-activated carbon of high surface area produced from coconut shell: Kinetics and equilibrium studies from the methylene blue adsorption. Chem. Eng. J., 174 (2011) 117–125.
[12] A.A. Hassan, Removal of reactive red 3B from aqueous solution by using treated orange peel, Int. J. Civ. Eng. Technol., 5 (2014) 160–169.
[13 K.Y. Foo, B.H. Hameed, Preparation, characterization and evaluation of adsorptive properties of orange peel based activated carbon via microwave induced K_2CO_3 activation, Bioresour. Technol., 104 (2012) 679–686.
[14] K.Y. Foo, B.H. Hameed, Potential of jackfruit peel as precursor for activated carbon prepared by microwave induced NaOH activation, Bioresour. Technol., 112 (2012) 143–150.
[15] K.Y. Foo, B.H. Hameed, Factors affecting the carbon yield and adsorption capability of the mangosteen peel activated carbon prepared by microwave assisted K_2CO_3 activation, Chem. Eng. J., 180 (2012c) 66–74.
[16] K.Y. Foo, B.H. Hameed, Porous structure and adsorptive properties of pineapple peel based activated carbons prepared via microwave assisted KOH and K_2CO_3 activation, Microporous Mesoporous Mater., 148 (2012) 191–195.

[17] S. Dutta, A. Bhattacharyya, A. Ganguly, S. Gupta, S. Basu, Application of response surface methodology for preparation of low-cost adsorbent from citrus fruit peel and for removal of methylene blue, Desalination, 275 (2011) 26–36.
[18] A.C. Arampatzidou, E.A. Deliyanni, Comparison of activation media and pyrolysis temperature for activated carbons development by pyrolysis of potato peels for effective adsorption of endocrine disruptor bisphenol-A, J. Colloid Interface Sci., 466 (2016) 101–112
[19] V.O. Njoku, K.Y. Foo, M. Asif, B.H. Hameed, Preparation of activated carbons from rambutan (Nephelium lappaceum) peel by microwave-induced KOH activation for acid yellow 17 dye adsorption, Chem. Eng. J., 250(2014) 198–204.
[20] M.A. Ahmad, N.A.A. Puad, O.S. Bello, Kinetic, equilibrium and thermodynamic studies of synthetic dye removal using pomegranate peel activated carbon prepared by microwave-induced KOH activation, Water Resour. Ind., 6 (2014) 18–35.
[21] Y.Y. Pei, J.Y. Liu (2011) Adsorption of Pb^{2+} in wastewater using adsorbent derived from grapefruit peel, Adv. Mater. Res., 391–392 (2011) 968–972.
[22] H.I. Owamah, Biosorptive removal of Pb(II) and Cu(II) from wastewater using activated carbon from cassava peels, J. Mater. Cycles Waste Manage., 16 (2014) 347–358.
[23] R. Pandey, N.G. Ansari, R.L. Prasad, R.C. Murthy, Removal of Cd(II) ions from simulated wastewater by HCl modified Cucumis sativus peel: equilibrium and kinetic study, Air Soil Water Res., 7 (2014) 93–101.
[24] O.S. Bello, M.A. Ahmad, B. Semire, Scavenging malachite green dye from aqueous solutions using pomelo (Citrus grandis) peels: kinetic, equilibrium and thermodynamic studies, Desal. Water Treat., 56 (2015) 521–535.
[25] K. Amela, M.A. Hassen, D. Kerroum, Isotherm and kinetics study of biosorption of cationic dye onto banana peel. Energy Procedia., 19 (2012) 286–295.
[26] P. Singh, P. Raizada, D. Pathania, G. Sharma, P. Sharma, Microwave induced KOH activation of guava peel carbon as an adsorbent for congo red dye removal from aqueous phase, Indian J. Chem. Technol., 20 (2013) 305–311.
[27] D.Z. Husein, Adsorption and removal of mercury ions from aqueous solution using raw and chemically modified Egyptian mandarin peel, Desalin. Water Treat., 51 (2013) 6761–6769.
[28] S.M.V. Palmeira, L.M. Gois, L.D. Souza, Extraction of phenolic compounds from mango peels, Latin. Am. Appl. Res., 42 (2012) 77–81.
[29] K. Bandyopadhyay, C. Chakraborty, S. Bhattacharyya, Fortification of mango peel and kernel powder in cookies formulation. J. Academia Indust. Res., 2 (2014) 661–664.
[30] H.J.Y. Kim, H. Moon, D. Kim, M. Lee, H. Cho, Y.S. Cho, M.A. Kim, S.K. Cho, Antioxidant and antiproliferative activities of mango (Mangifera indica L.) flesh and peel. Food Chem., 121 (2010) 429–436.
[31] I.S. Ashoush, M.G.E. Gadallah, Utilization of Mango peels and seed kernels powders as sources of phyto chemicals in biscuit. World J. Dairy Food Sci., 6 (2011) 35–42.
[32] A.H. Jawad, A.F.M. Alkarkhi, O.C. Jason, A.M. Easa, N.A.N. Norulaini, Production of the lactic acid from mango peel waste – Factorial experiment. J. King Saud Univ. Sci., 25 (2013) 39–45.
[33] K.V. Kumar, A. Kumaran, Removal of methylene blue by mango seed kernel powder. Biochem. Eng. J., 27 (2005) 83–93.
[34] M.M. Dávila-Jiménez, M.P. Elizalde-González, V. Hernández-Montoy, Performance of mango seed adsorbents in the adsorption of anthraquinone and azo acid dyes in single and binary aqueous solutions. Bioresour. Technol., 100 (2009) 6199–6206.
[35] W.S. Alencar, E. Acayanka, E.C. Lima, B. Royer, F.E. de Souza, J. Lameira, C.N. Alves, Application of *Mangifera indica* (mango) seeds as a biosorbent for removal of Victazol Orange 3R dye from aqueous solution and study of the biosorption mechanism. Chem. Eng. J., 209 (2012) 577–588.
[36] K. Munusamy, R.S. Somani, H.C. Bajaj, Breakthrough adsorption studies of mixed gases on mango (*Mangifera indica* L.) seed shell derived activated carbon extrudes. J. Environ. Chem. Eng., 3 (2015) 2750–2759.
[37] M.P. Elizalde-González, V. Hernández-Montoya, Characterization of mango pit as raw material in the preparation of activated carbon for wastewater treatment. Biochem. Eng. J., 36 (2007) 230–283.
[38] F.C. Wu, R.L. Tseng, C.C. Hu. Comparisons of pore properties and adsorption performance of KOH-activated and steam-activated carbons. Microporous Mesoporous Mater., 80 (2005) 95–106.
[39] Ö. Gerçel, A. Özcan, A.S. Özcan, H.F. Gerçel. Preparation of activated carbon from a renewable bio-plant of Euphorbia rigida by H_2SO_4 activation and its adsorption behavior in aqueous solutions. Appl. Surf. Sci., 253 (2007) 4843–4852.
[40] V.K. Garg, R. Kumar, R. Gupta. Removal of malachite green dye from aqueous solution by adsorption using agro-industry waste: a case study of Prosopis cineraria. Dyes Pigments, 62 (2004) 1–10.
[41] M. Auta, B.H. Hameed. Optimized waste tea activated carbon for adsorption of Methylene Blue and Acid Blue 29 dyes using response surface methodology. Chem. Eng. J., 175 (2011) 233–243.
[42] M. Ahmedna, W.E. Marshall, R.M. Rao, S.J. Clarke. Use of filtration and buffers in raw sugar colour measurements. J. Sci. Food Agric., 75 (1997) 109–116.
[43] F.A. Adekola, H.I. Adegoke. Adsorption of blue-dye on activated carbons produced from rice husk, coconut shell and coconut coir pith. Ife J. Sci., 7 (2005) 151–157.
[44] ASTM Standard, Standard Test Method for Total Ash Content of Activated Carbon, Designation D2866-94, 2000.
[45] Lubrizol standard test method, Iodine value, test procedure AATM 1112-01, October 16 (2006).
[46] M.V. Lopez-Ramon, F. Stoeckli, C. Moreno-Castilla, F. Carrasco-Marin, On the characterization of acidic and basic surface sites on carbons by various techniques, Carbon, 37 (1999) 1215–1221.
[47] R. Gnanasambandam, A. Protor. Determination of pectin degree of esterification by diffuse reflectance Fourier transforms infrared spectroscopy. Food Chem., 68 (2000) 327–332.
[48] M. Benadjemia, L. Millière, L. Reinert, N. Benderdouche, L. Duclaux, Preparation, characterization and Methylene Blue adsorption of phosphoric acid activated carbons from globe artichoke leaves, Fuel Process. Technol., 92 (2011) 1203–1212.
[49] G.E. Nascimento, M.M.M.B. Duarte, N.F. Campos, O.R.S. Rocha, V.L. Silva. Adsorption of azo dyes using peanut hull and orange peel: a comparative study. Environ. Technol., 35 (2014) 1436–1453.
[50] S. Chakraborty, S. Chowdhury, P.D. Saha. Adsorption of crystal violet from aqueous solution onto NaOH-modified rice husk. Carbohydr. Polym., 86 (2011) 1533–1541.
[51] H. Lata, V.K. Garg, R.K. Gupta. Removal of a basic dye from aqueous solution by adsorption using *Parthenium hysterophorus*: An agricultural waste. Dyes Pigments 74 (2007) 653–658.
[52] B. Royer, N.F. Cardoso, E.C. Lima, J.C.P. Vaghetti, R.C. Veses. Applications of Brazalin pine-fruit shell in natural and carbonized forms as adsorbents to removal of methylene blue from aqueous solutions: kinetics and equilibrium study. J. Hazard. Mater., 164 (2009) 1213–1222.
[53] A.E. Ofomaja. Sorption dynamics and isotherm studies of methylene blue uptake on to palm kernel fibre. Chem. Eng. J., 126 (2007) 35–43.
[54] S. Lagergren, About the theory of so called adsorption of soluble substances, kungliga SvenskaVetenskapsakademiens, Handlingar, Band, 24, No. 04 (1898) 1–39.
[55] Y.S. Ho, G. McKay, Pseudo-second-order model sorption processes, Process Biochem., 34 (1999) 451–465.
[56] I. Langmuir, The adsorption of gases on plane surfaces of glass, mica and platinum, J. Am. Chem. Soc., 40 (1918) 1361–1403.
[57] H.M.F. Freundlich. Over the adsorption in solution. J. Phys. Chem., 57 (1906) 385–470.
[58] M.J. Temkin, V. Pyzhev, Recent modifications to Langmuir isotherms, Acta Physiochim. USSR, 12 (1940) 217–222.

[59] S. Karagoz, T. Tay, S. Ucar, M. Erdem. Activated carbons from waste biomass by sulfuric acid activation and their use on methylene blue adsorption. Bioresour. Technol., 99 (2008) 6214–6222.
[60] Y.S. Ho R. Malaryvizhi, N. Sulochana. Equilibrium isotherm studies of methylene blue adsorption onto activated carbon prepared from Delonix regia pods. J Environ Prot Sci., 3:1 (2009) 1–6.
[61] D. Pathania, S. Sharma, P. Singh. Removal of methylene blue by adsorption onto activated carbon developed from Ficus carica bast. Arab. J. Chem., http://doi.org/10.1016/j.arabjc.2013.04.021.
[62] L.W. Low, T.T. Teng, A. Ahmad, N. Morad, Y.S. Wong. A novel pretreatment method of lignocellulosic material as adsorbent and kinetic study of dye waste *adsorption*. Water, Air, Soil Pollut., 218 (2011) 293–306.
[63] A.H. Jawad, R.A. Rashid, M.A.M. Ishak, L.D. Wilson. Adsorption of methylene blue onto activated carbon developed from biomass waste by H_2SO_4 activation: kinetic, equilibrium and thermodynamic studies. Desal. Water Treat., 57(52) (2016) 25194–25206.
[64] G. Karaçetin, S. Sivrikaya, M. Imamoğlu. Adsorption of methylene blue from aqueous solutions by activated carbon prepared from hazelnut husk using zinc chloride. J. Anal. Appl. Pyrolysis., 110 (2014) 270–276.
[65] R.A. Rashid, A.H. Jawad, M.A.M. Ishak, N.N. Kasim. KOH-activated carbon developed from biomass waste: adsorption equilibrium, kinetic and thermodynamic studies for Methylene blue uptake. Desal. Water Treat., 57(56) (2016) 27226–27236.
[66] Y. Yu, Y.Y. Zhuang, Z.H. Wang. Adsorption of water-soluable dye onto functionalized resin, J. Colloid Interf. Sci., 242 (2001) 288–293.
[67] D.D. Asouhidou, K.S. Triantafyllidis, N.K. Lazaridis, K.A. Matis, S.S. Kim, T.J. Pinnavaia. Sorption of reactive dyes from aqueous solutions by ordered hexagonal and disordered mesoporous carbons. Micropor. Mesopor. Mater., 117 (2009) 257–267.
[68] T. Calvete, E.C. Lima, N.F. Cardoso, J.C.P. Vaghetti, S.L.P. Dias, F.A. Pavan. Application of carbon adsorbents prepared from Brazilian-pine shell for the removal of reactive orange 16 from aqueous solution: Kinetic, equilibrium, and thermodynamic studies. J. Environ. Manage., 91 (2010) 1695–1706.